Supplementary Information (SI) for Journal of Materials Chemistry A.

Supplementary information

Multifunctional broadband emitters based on rare earth phosphors for all-weather and efficient radiative cooling and energy saving

Qinglong Hu[1], Ruiming Tan[1], Pengjie Zhong[1], Keyu Han[1]*, Yinyan Li[2], Peng Xue[3]*, and Gongxun Bai[1]*

[1] College of Optical and Electronic Technology, China Jiliang University, Hangzhou 310018, China

[2] Key Laboratory of Rare Earth Optoelectronic Materials and Devices of Zhejiang Province, China Jiliang University, Hangzhou 310018, China

[3] Beijing Key Laboratory of Green Building Environment and Energy Saving Technology, Beijing University of Technology, Beijing 100124, China

* Corresponding author: hanky@cjlu.edu.cn (K Han), xp@bjut.edu.cn (P. Xue), baigx@cjlu.edu.cn (G Bai)

Supporting Texts:

1. Calculation formula of net radiant cooling power.

2. Calculation of mean solar reflectance and emissivity.

Supporting Figures:

Supporting Tables:

Table S1. Mass ratio of each substance in preparation of the SM film.

Table S2. Optical and radiative cooling properties of SM film and WR film.

Table S3. Performance comparison of the SM film and WR film with other work reports.

Supporting Text:

Calculation formula of net radiant cooling power.[1,2]

The following formula (1) is the calculation formula of the net radiant cooling power. Among them, P_{rad} is the power radiated outward by the radiator cooling, P_{atm} is the atmospheric long-wave radiation power absorbed by the radiation cooler, P_{sun} is the absorbed solar radiation, and P_{con} refers to the non-radiative heat transfer power between the radiation cooler and the surrounding environment, that is, heat conduction and heat convection.

$$P_{cooling}(T)=P_{rad}(T)-P_{atm}-P_{sun}-P_{con} \quad (1)$$

Where $A_{RC}(\lambda,\theta)$ is the absorption spectrum of the film, θ means the the angle of incidence of sunlight on the sample, it assumes that the sunlight is at normal incidence ,i.e., $\theta = 0°$. $A_{RC}(\lambda,\theta)$ can be obtained from the reflectance spectrum (R) and transmittance spectrum (T) in the range of 0.3-2.5 μm, $A_{RC}(\lambda,\theta_{sun}) = 1-R(\lambda)-T(\lambda)$. $I_{bb}(\lambda,T) = \frac{2hc^2}{\lambda^5(e^{hc/\lambda KT}-1)}$ is the radiation power spectrum of the blackbody at the temperature T, $I_{atm}(\lambda)=\int I_{bb}(\lambda, T)\varepsilon_s(\Omega, \lambda)\, \varepsilon_{atm}(\Omega, \lambda)d\lambda$ is the downward long-wave radiation flux spectrum of the atmosphere. $\varepsilon_s(\Omega, \lambda)$ is the emissivity of the surface as a function of direction and wavelength. $\varepsilon_{atm}(\Omega, \lambda)$ is the emissivity of atmosphere as a function of direction and wavelength. where P_{abs} is the absorbed solar irradiance by the film, and P_{fluo} can be expressed as follow $P_{fluo}=\alpha\beta\Phi\int E_{fluo}(\lambda)A_{RC}(\lambda)I_{sun}(\lambda)d(\lambda)$. Where I_{sun} is the solar spectrum and $E_{fluo}(\lambda)$ is the excitation spectrum of SM film. α is the ratio of fluorescence excitation, β is the ratio of fluorescence emission energy, Φ is the fluorescence quantum yield of SM film. Where $h_c=Q/(S*\Delta T)$ is the non-radiation heat transfer coefficient of the radiation cooling device and the surrounding environment, and T and T_a are the device temperature and the surrounding environment temperature respectively.

The detailed formula is as follows:

$$P_{rad}(T)=\int A_{RC}(\lambda,\theta)\, I_{bb}(\lambda,T)d\lambda \quad (2)$$

$$P_{atm}=\int A_{RC}(\lambda)\, I_{atm}(\lambda)d\lambda \quad (3)$$

$$P_{sun}=P_{abs}-P_{fluo} \quad (4)$$

$$P_{con}=h(T-T_a) \quad (5)$$

Calculation of mean solar reflectance and emissivity.[3]

$$\bar{R}_{solar}=\frac{\int_{0.3\,\mu m}^{2.5\,\mu m} I_{AM1.5}(\lambda)R(\lambda)d(\lambda)}{\int_{0.3\,\mu m}^{2.5\,\mu m} I_{AM1.5}(\lambda)d(\lambda)} \quad (6)$$

$$E_{IR} = \frac{\int_{2.5\,\mu m}^{20\,\mu m} I_{bb}(\lambda,T)E(\lambda)d(\lambda)}{\int_{2.5\,\mu m}^{20\,\mu m} I_{bb}(\lambda,T)d(\lambda)} \qquad (7)$$

$$E_{AWR} = \frac{\int_{8\,\mu m}^{13\,\mu m} I_{bb}(\lambda,T)E(\lambda)d(\lambda)}{\int_{8\,\mu m}^{13\,\mu m} I_{bb}(\lambda,T)d(\lambda)} \qquad (8)$$

Supporting Figures:

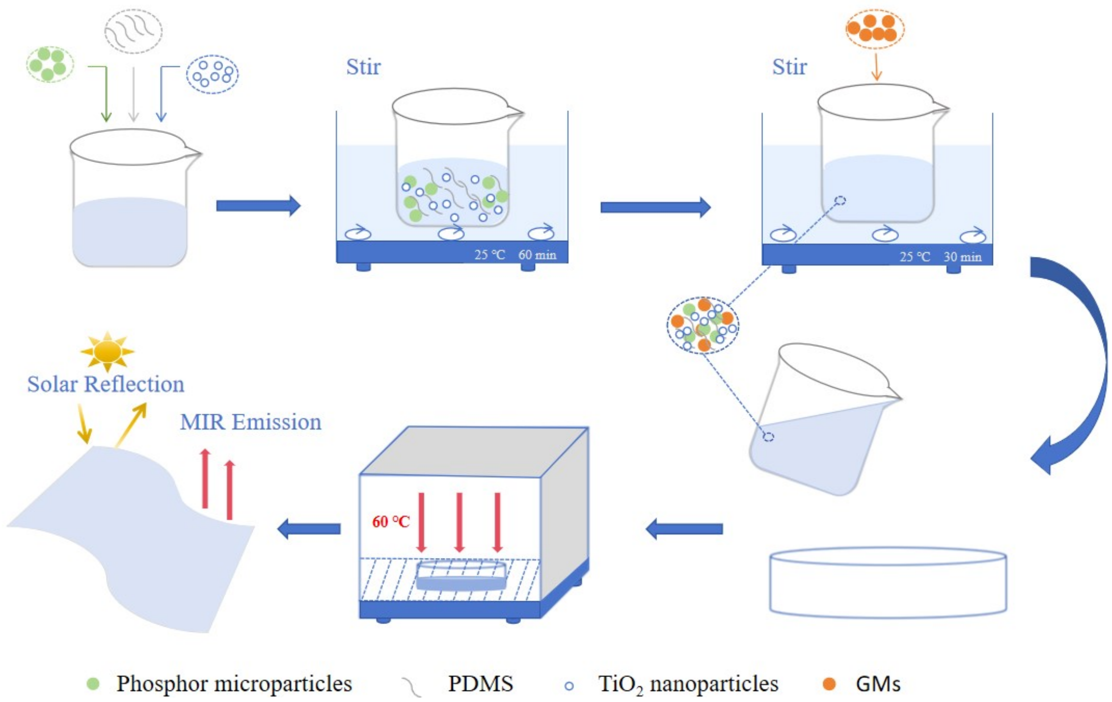

Figure S1. Schematic illustration showing the fabrication process of SM film and WR film using sol-gel method.

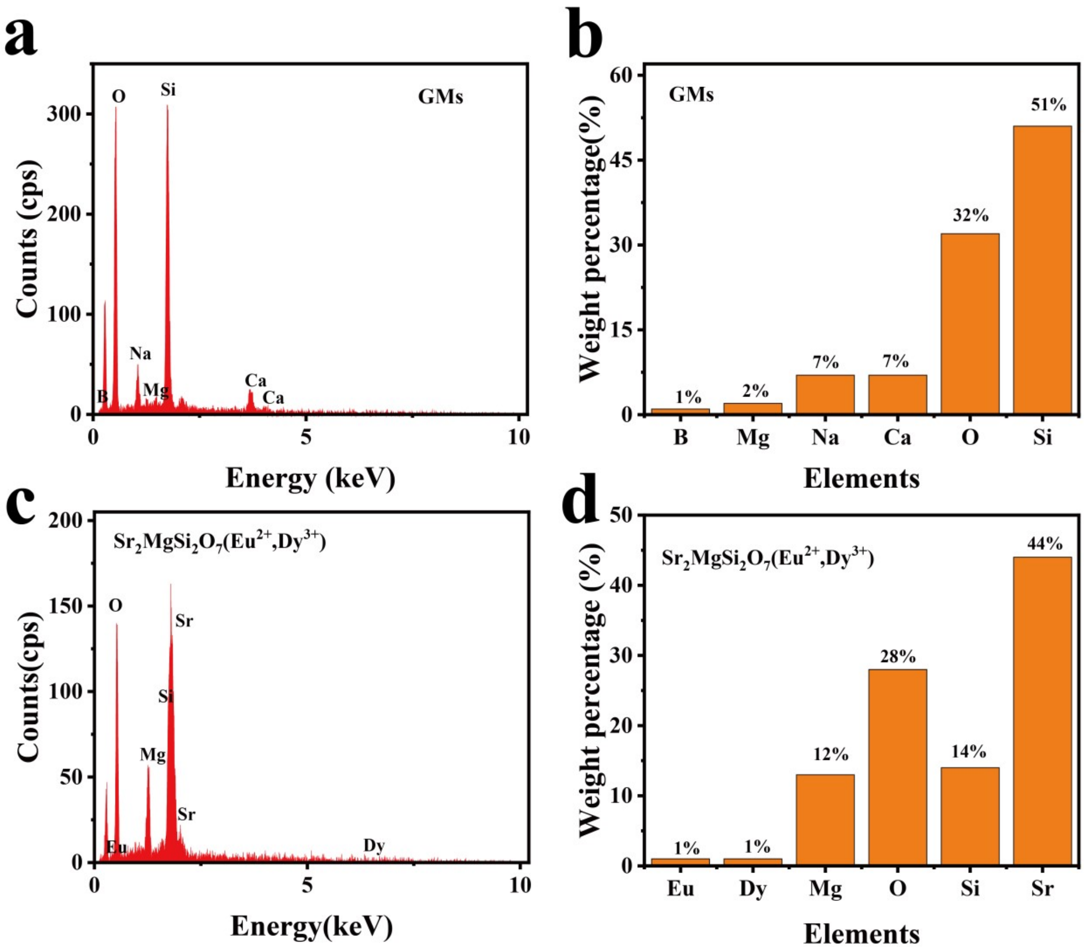

Figure S2. EDS energy spectra and ratio number plots of each element. (a) EDS spectra of GMs particles. (b) Ratio data of each element of GMs. (c) EDS spectra of $Sr_2MgSi_2O_7(Eu^{2+}, Dy^{3+})$ particles. (d) Ratio data plot of each element of $Sr_2MgSi_2O_7(Eu^{2+}, Dy^{3+})$.

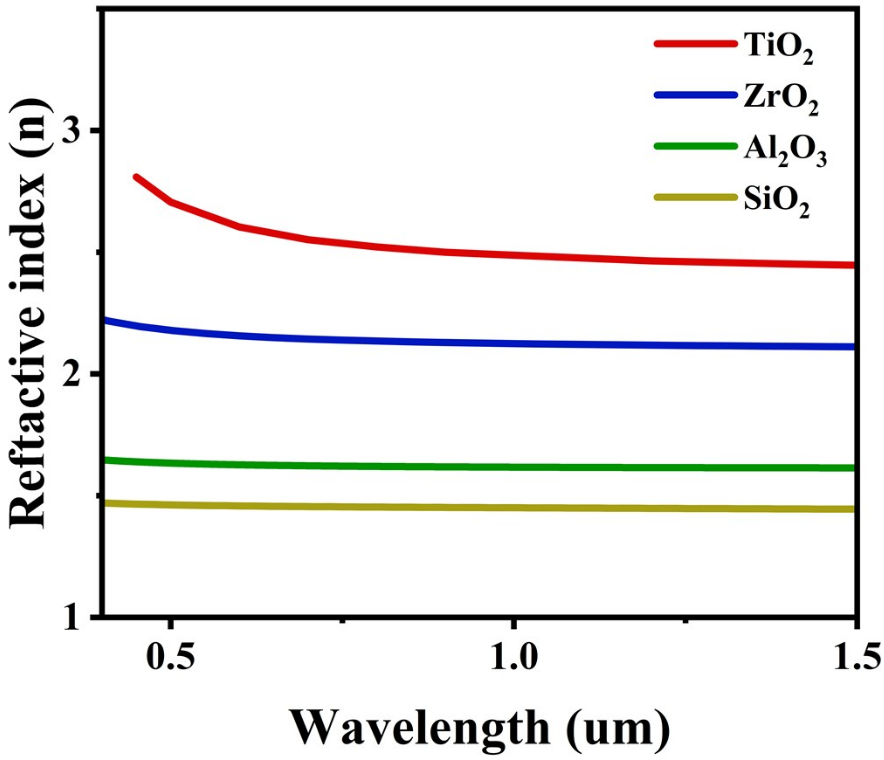

Figure S3. The Scattering efficiency diagram of four different particles: TiO_2, ZrO_2, Al_2O_3, SiO_2.

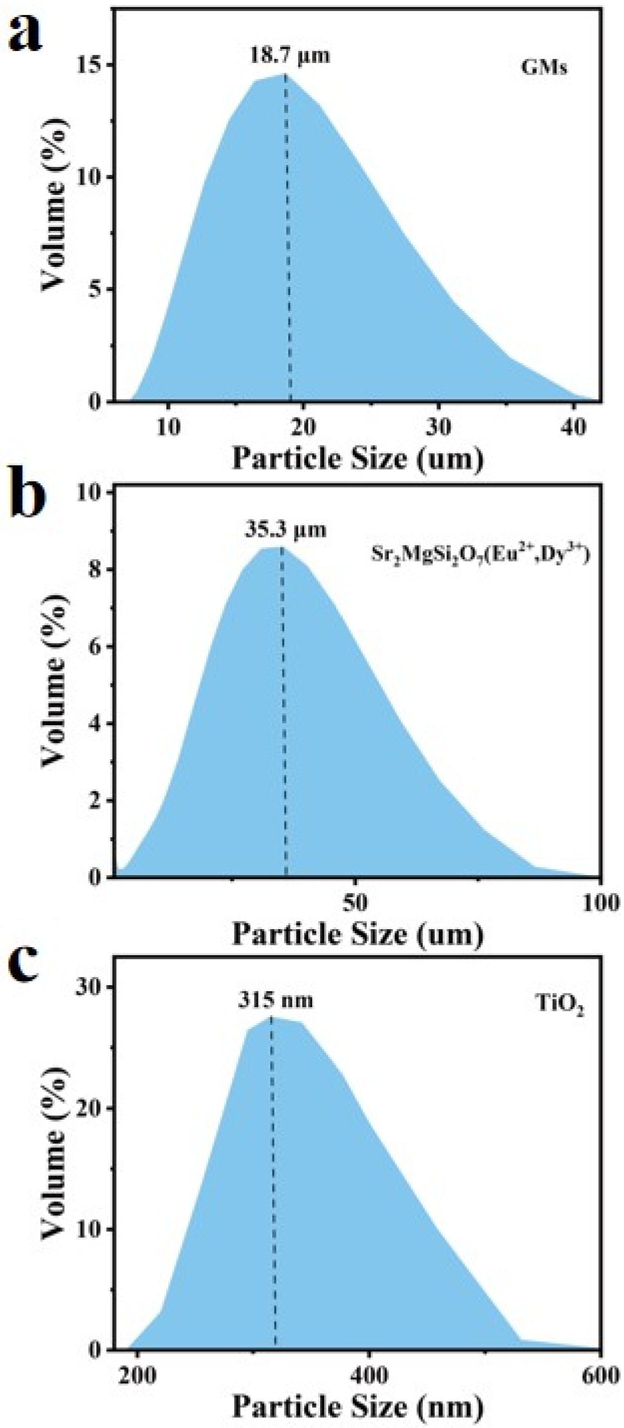

Figure S4. The particle size analysis diagram of (a) GMs, (b) REPs and (c) TiO_2. Plot of particle size analysis data for GMs (5-40 μm). Plot of particle size analysis data for REPs (5-100 μm). Plot of TiO_2 particle size analysis data (200-600 nm)

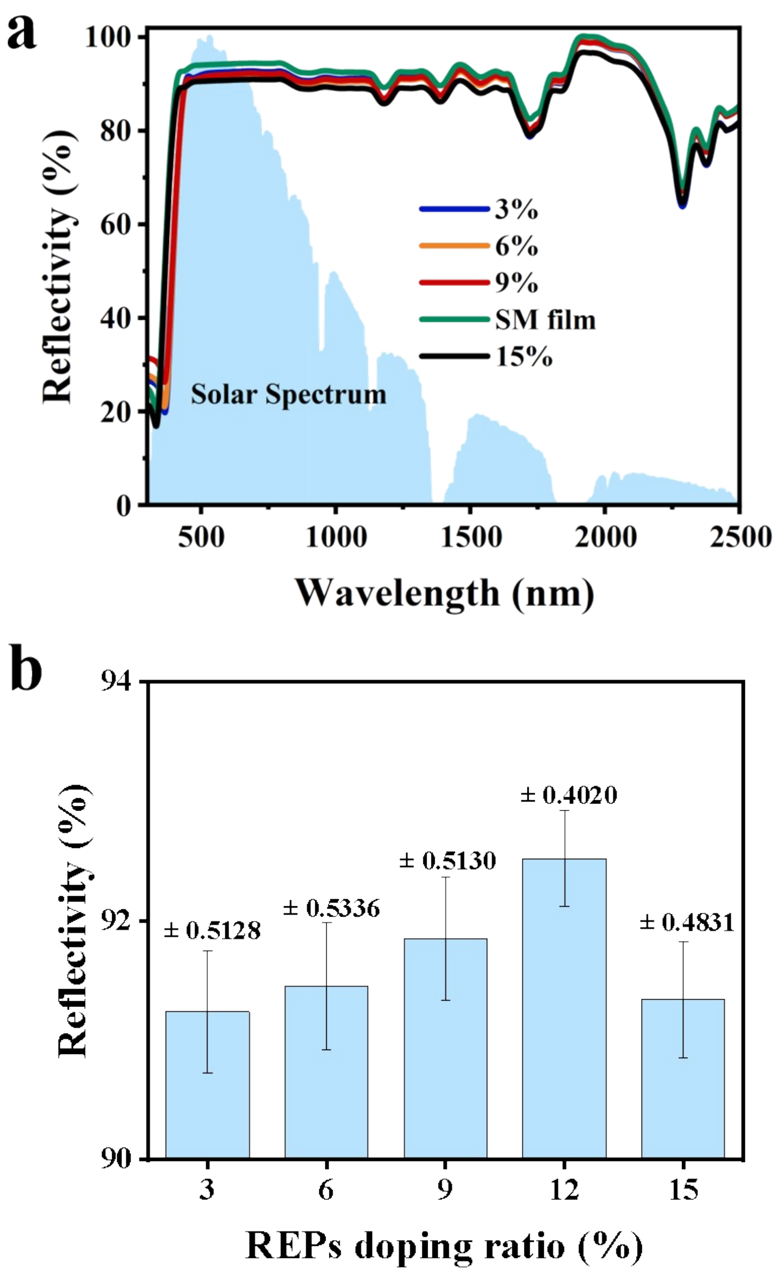

Figure S5. Reflection data diagram and error analysis diagram. (a) Reflectance data of SM films prepared with varying proportions REPs. (b) Error analysis diagram of different REPs incorporated proportional reflection data.

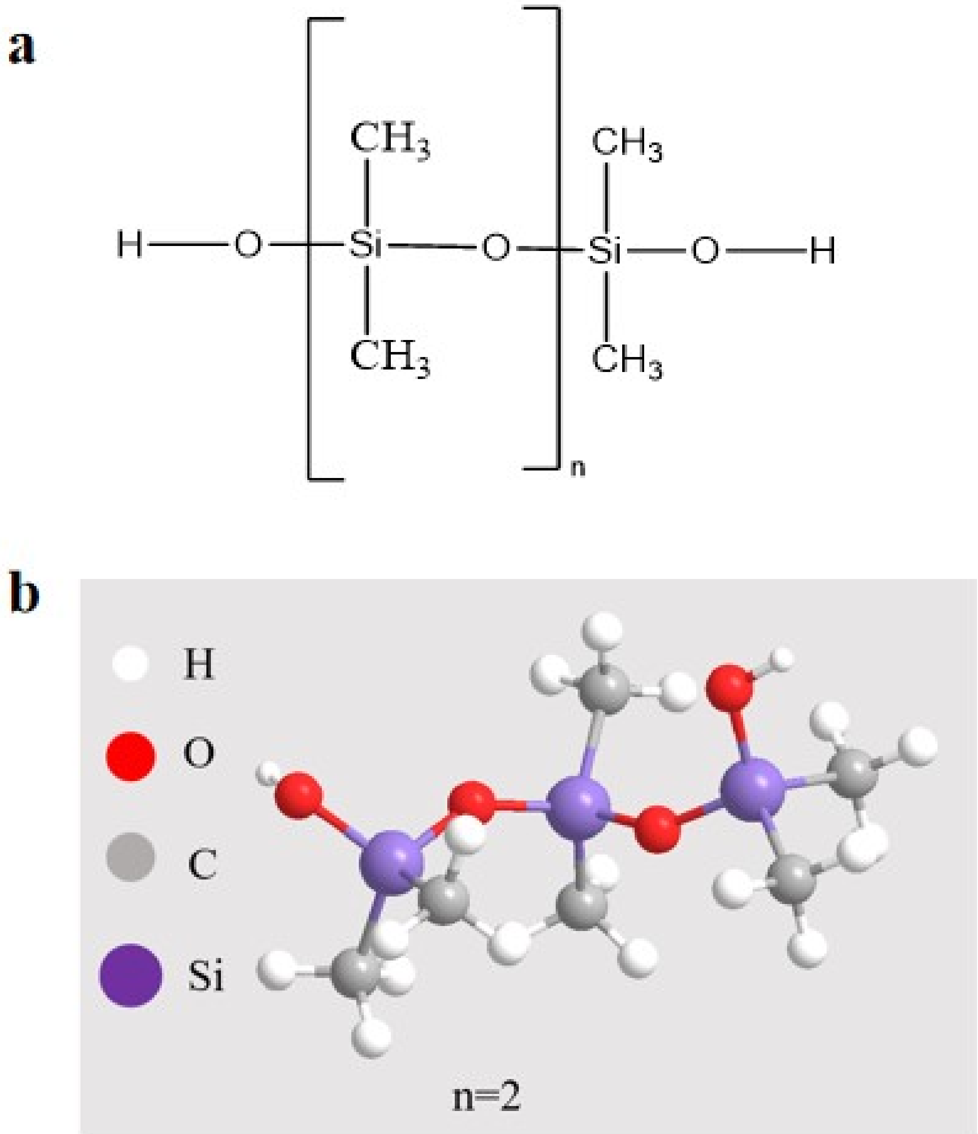

Figure S6. Schematic diagram of the PDMS structure. (a) Chemical structural formula of PDMS. (b) Diagram of the PDMS ball-and-stick model.

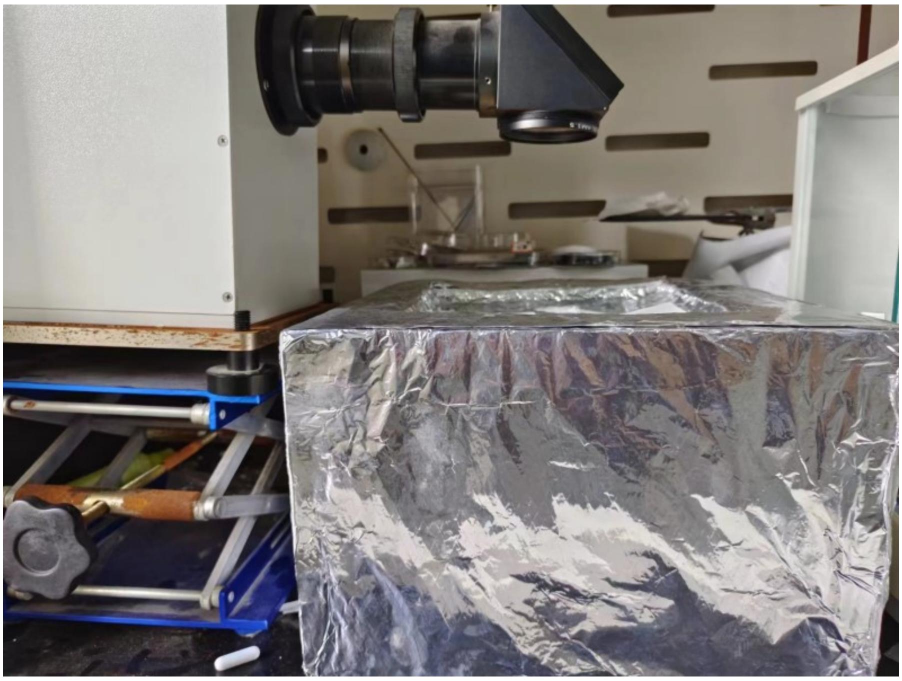

Figure S7. Indoor temperature measuring device physical demonstration.

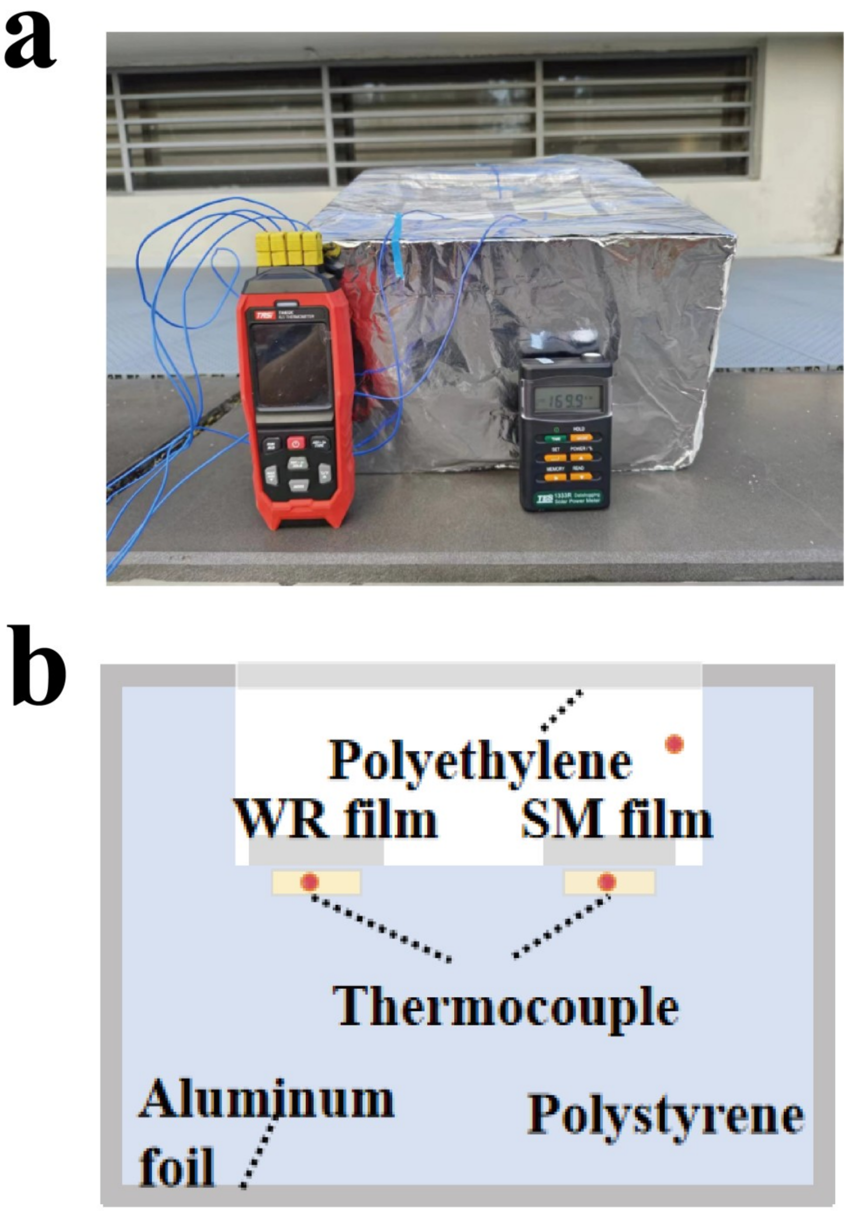

Figure S8. Schematic diagram of the outdoor cooling unit. (a) Physical representation of the outdoor cooling unit. (b) Schemat222ic diagram of the outdoor cooling device .

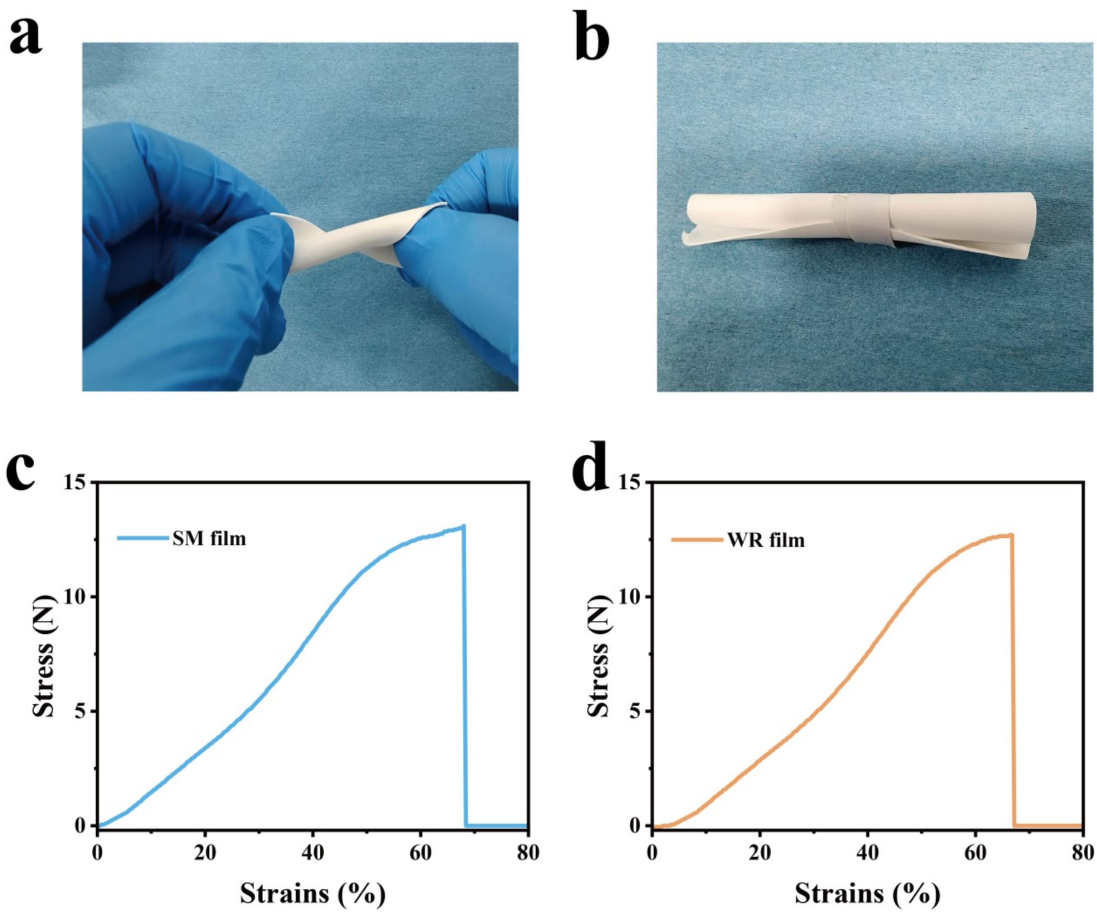

Figure S9. Sample mold flexibility and tensile test. (a-b) Flexibility test of the sample film by twisting and rolling. (c-d) The tensile properties curve of the sample film obtained by instrument (Sample film dimensions: 30*20 mm). The maximum tensile strength of the SM film reached 13.1 N, while the maximum tensile strength of the WR film reached 12.7 N.

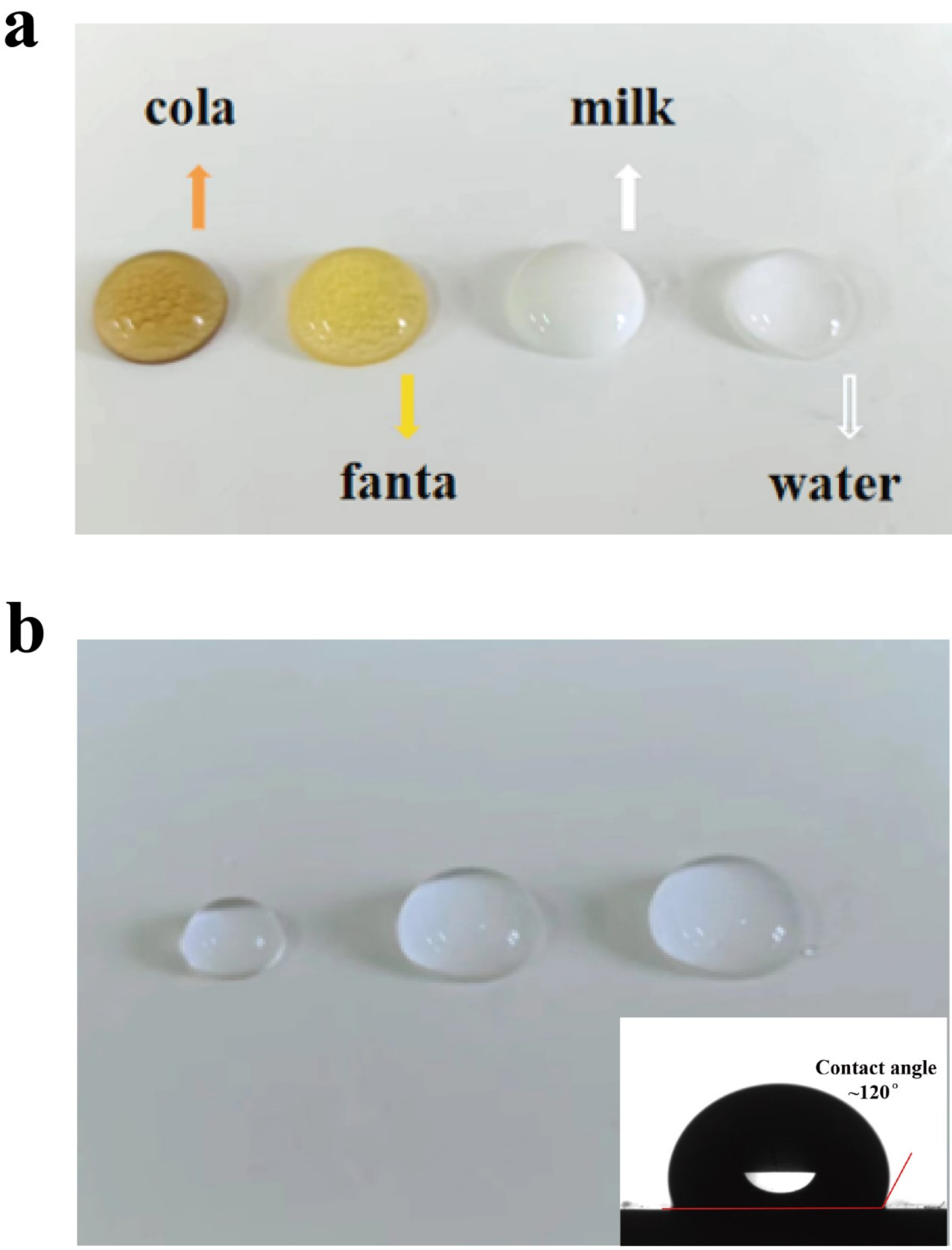

Figure S10. SM film are tested for hydrophobicity with variousliquids. (a) Hydrophobicity test conducted with four different liquids (cola, fanta, milk andwater) and the sample moulds. (b) Hydrophobicity test performed with different volumes of liquid and sample mould.

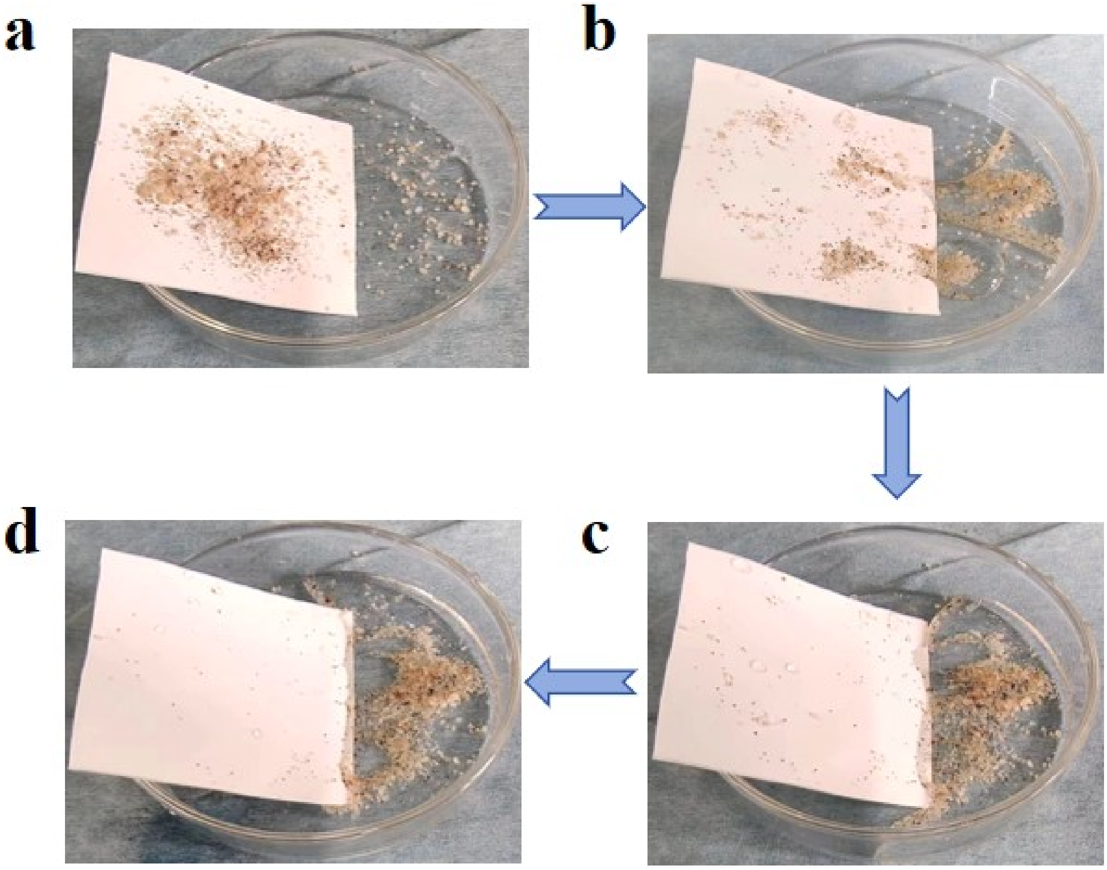

Figure S11. Self-cleaning test of SM film with sand. (a-d) Sprinkle sand randomly on the surface of SM film, and then rinse SM film with dropper dripping water. In this way, the self-cleaning performance of SM film is tested.

Table S1. Mass ratio of each substance in preparation of the SM film.

Compositions Samples	PDMS	GMs	TiO_2	REPs
P1	60%	10%	27%	3%
P2	60%	10%	24%	6%
P3	60%	10%	21%	9%
SM film	**60%**	**10%**	**18%**	**12%**
P5	60%	10%	15%	15%

Table S2. Optical and radiative cooling properties of SM film and WR film.

Samples	**SM film**	WR film
Reflectivity	**0.93**	0.911
Emissivity	**0.95**	0.926
ΔT (°C)	**8.26**	6.42

Table S3. Performance comparison of the SM film and WR film with other work reports.

Samples	Reflectivity	Emissivity	ΔT (°C)	Ref.
Fluorescent coatings	0.898	0.900	7	1
Shish-kebab superstructure films	0.830	0.870	8.2	4
Self-Cleaning polymer composites	0.921	0.75	7.8	5
Polymethyl methacrylate films	0.850	0.984	8.1	6
Cellulose-based fabric	0917	0.900	7.5	7
Scalable-manufactured dual-layer coating	0.880	0.920	3.6	8
A tandem radiative/evaporative cooler	0.930	0.800	10	9
Bio-RC film	0.953	0.934	3.7	10
SM film	**0.93**	**0.95**	**8.26**	**This work**
WR film	0.911	0.926	6.42	Comparative work

References

1 X. Xue, M. Qiu, Y. Li, Q. Zhang, S. Li, Z. Yang, C. Feng, W. Zhang, J. Dai, D. Lei, W. Jin, L. Xu, T. Zhang, J. Qin, H. Wang, S. Fan, *Adv. Mater*. 2020, **32**, 1906751.

2 J. Li, Y. Fu, J. Zhou, K.Yao, X. Ma, S. Gao, Z. Wang, J. Dai, D. Lei, X. Yu, *Sci. Adv.,* 2023, **9**, eadg1837.

3 M. Yang, H. Zhong, T. Li, B. Wu, Z. Wang, D. Sun, *ACS Nano*, 2023**,** **17**, 1693–1700.

4 X. Liu, Y. Li, Y. Pan, Z. Zhou, Z. Zhai, C. Liu, C. Shen, *ACS Appl. Mater. Interfaces,* 2023, **15**, 17188-17194.

5 K. Zhou, X. Yan, S. J. Oh, G. Padilla-Rivera, H. Kim, D. Cropek, N. Miljkovic, L. Cai, *Nano Lett*., 2023, **23**, 3669–3677.

6 G. Qi, X. Tan, Y. Tu, X. Yang, Y. Qiao, Y. Wang, J. Geng, S. Yao, X. Chen, *ACS Appl. Mater. Interfaces,* 2022, **14**, 31277–31284.

7 Y. Zhang, W. Zhu, C. Zhang, J. Peoples, X. Li, A. L. Felicelli, X. Shan, D. M. Warsigner, T. Borca-Tasciuc, X. Ruan, T. Li, *Nano Lett.,* 2022, **22**, 2618–2626.

8 S. Wang, Y. Wang, Y. Zou, G. Chen, J. Ouyang, D. Jia, Y. Zhou, *ACS Appl. Mater. Interfaces,* 2021, **13**, 21888–21897.

9 J. Li, X. Wang, D. Liang, N. Xu, B. Zhu, W. Li, P. Yao, Y. Jiang, X. Min, Z. Huang, S. Zhu, S. Fan, J. Zhu, *Sci. Adv.,* 2022, **8**, eabq0411.

10 S. Shi, P. Lv, C. Valenzuela, B. Li, Y. Liu, L. Wang, W. Feng, Small, 2023, **39**, 2301957.